Available online at www.sciencedirect.com

SCIENCE DIRECT®

Journal of Solid State Chemistry 177 (2004) 3927–3933

JOURNAL OF
SOLID STATE
CHEMISTRY

www.elsevier.com/locate/jssc

Synthesis, band structure, and optical properties of $Ba_2ZnV_2O_8$

D.-G. Chen, W.-D. Cheng*, D.-S. Wu, H. Zhang, Y.-C. Zhang, Y.-J. Gong, Z.-G. Kan

Fujian Institute of Research on the Structure of Matter, State Key Laboratory of Structural Chemistry,
The Graduate School of the Chinese Academy of Sciences, Fuzhou, Fujian 350002, China

Received 8 June 2004; received in revised form 5 July 2004; accepted 8 July 2004
Available online 18 September 2004

Abstract

A novel compound $Ba_2ZnV_2O_8$ has been synthesized in high temperature solution reaction and its crystal structure has been characterized by means of single crystal X-ray diffraction analysis. It crystallizes in monoclinic system and belongs to space group $P2_1/c$ with $a = 7.9050(16)$, $b = 16.149(3)$, $c = 6.1580(12)$ Å, $\beta = 90.49(3)$. It builds up from 1-D branchy chains of $[ZnV_2O_8^{4-}]_\infty$, and the Ba^{2+} cations are located in the space among these chains. The IR spectrum, ultraviolet-visible diffuse reflection integral spectrum and fluorescent spectra of this compound have been investigated. The calculated results of energy band structure by the density functional theory method show that the solid-state compound of $Ba_2ZnV_2O_8$ is an insulator with direct band gap of 3.48 eV. The calculated total and partial density of states indicate that the top valence bands are contributions from the mixings of O-2*p*, V-3*d*, and Zn-3*d* states and low conduction bands mostly originate from unoccupied antibonding states between the V-3*d* and O-2*p* states. The V–O bonds are mostly covalence characters and Zn–O bonds are mostly ionic interactions, and the ionic interaction strength is stronger between the Ba–O than between the Zn–O. The refractive index of n_x, n_y, and n_z is estimated to be 1.7453, 1.7469, and 1.7126, respectively, at wavelength of 1060 nm for $Ba_2ZnV_2O_8$ crystal.

Keywords: Crystal structure; Energy band; Orthovanadate; Optical properties

1. Introduction

During the past decades, numerous investigations have been published about the compounds found in ternary systems $AO–M^{II}O–V_2O_5$ (A = Mg, Sr, Ba; M^{II} = Ni, Mn, Cu, Zn). For example, many compounds of the $AM_2^{II}V_2O_8$ family were synthesized and the magnetic properties of these compounds were studied [1–5]. However, the compounds with formula of $A_2M^{II}V_2O_8$ are rarely found in these systems. To our knowledge, only $Mg_2CuV_2O_8$ and $Mg_2NiV_2O_8$ were found [6,7]. On the other hand, the vanadates containing zinc in combination with alkaline-earth metals are inadequately studied [8–10]. In this paper, we report the synthesis of a new compound $Ba_2ZnV_2O_8$ (**1**) in high temperature solution reaction and the determination of its crystal structures by single crystal X-ray diffraction (XRD). Since many zinc compounds usually have good luminescent properties, the ultraviolet-visible diffuse reflection integral spectrum (UV-Vis DRIS) and fluorescent spectra of the title compound have been studied. Furthermore, the calculations of crystal energy band structure and optical response functions have done in order to understand the chemical bonding properties and electronic origins of optical transition for $Ba_2ZnV_2O_8$ crystal.

2. Experimental and computional procedures

2.1. Synthesis and analysis

Polycrystalline samples of $Ba_2ZnV_2O_8$ were synthesized by solid-state reactions of stoichiometric amounts of $Ba(NO_3)$ (Analytical reagent), ZnO (Analytical

---

*Corresponding author. Fax: +86-591-371-4946
E-mail address: cwd@ms.fjirsm.ac.cn (W.-D. Cheng).

0022-4596/$ - see front matter © 2004 Elsevier Inc. All rights reserved.
doi:10.1016/j.jssc.2004.07.017

reagent), and V_2O_5 (Analytical reagent). The mixtures were ground into fine powder in a mortar of agate under ethanol and heated at 773 K for 24 h in a platinum crucible, reground, and then allowed to react at 1133 K for 48 h with several intermediate grindings. The products were analyzed by powder XRD.

Single crystal of compound **1** was grown with the compound B_2O_3 as a flux. A solute-flux mixture, 4:1 by mass, was heated in a Pt crucible to 1153 K, cooled at 3 K/h to 1033 K, and then rapidly cooled to room temperature. The yellow needle like crystal was physically separated from the melt for structure determinations.

2.2. X-ray determination

Crystal data, collected reflections and parameters of the final refinement are reported in Table 1. Intensities data were collected using Siemens SMART CCD diffractometer with graphite-monochromated Mo-$K\alpha$ ($\lambda = 0.71073$ Å) radiation in the ω and φ scanning mode at room temperature. An empirical absorption correction was applied using SADABS program. The structure of the title compound was solved using direct methods and refined on F^2 by full-matrix least-squares methods using the SHELX97 program package [11]. The final $R_1 = 0.0516$ and $wR_2 = 0.1134$ for 1328 reflections ($I > 2\sigma(I)$) are acceptable, while the $R_1 = 0.0909$ and $wR_2 = 0.1339$ for all 2392 reflections are rather high, which may be caused by the $I < 2\sigma(I)$ reflections. The atom coordinates and thermal parameters are listed in Table 2. The selected bond distances and angles are listed in Table 3.

Table 1
Crystal data and structure refinement for $Ba_2ZnV_2O_8$

Formula	$Ba_2ZnV_2O_8$
Formula weight ($g\,mol^{-1}$)	569.93
Temperature (K)	293(2)
Wavelength (Å)	0.71073
Crystal system	Monoclinic
Space group	$P2_1/c$
Unit cell dimensions	$a = 7.9050(16)$ Å
	$b = 16.149(3)$ Å
	$c = 6.1580(12)$ Å
	$\beta = 90.49(3)°$
Volume, Z	786.1(3), 4
D_{calc} ($g\,cm^{-3}$)	4.816
μ (mm^{-1})	15.174
$F(000)$	1008
Crystal size (mm)	$0.22 \times 0.04 \times 0.04$
θ range (deg)	2.52∼25.10
Limiting indices	$-6 \leqslant h \leqslant 9$; $-19 \leqslant k \leqslant 17$; $-7 \leqslant l \leqslant 7$
Reflections collected	2392
Independent reflections	1328 ($R_{int} = 0.0662$)
Refinement method	Full-matrix least-squares on F^2
Weighting details	$w = 1[\sigma^2(F_0^2) + (0.0700P)^2 + 0.5000P]$ where $P = (F_o^2 + 2F_c^2)/3$
GOF	1.007
Final R indices [$I > 2\sigma(I)$]	$R_1 = 0.0516$, $wR_2 = 0.1134$
R indices (all data)	$R_1 = 0.0909$, $wR_2 = 0.1339$
Largest diff. peak and hole (e Å^3)	2.183 and −1.697

$R_1 = \sum ||F_{obs}| - |F_{calc}|| / \sum |F_{obs}|$,
$wR_2 = [\sum w(F_{obs}^2 - F_{calc}^2)^2 / \sum w(F_o^2)]^{1/2}$.

2.3. Physical measurement

Powder XRD data were obtained using Philips X'Pert-MPD diffractometer with Cu-$K\alpha$ radiation (1.5406). Fluorescent spectra were measured on an Edinburgh Instrument F920 fluorescent spectrometer using Xe lamp. The UV-Vis DRIS spectra were recorded on a Perkin-Elmer Lambda 900 UV-Vis spectrometer. The IR spectrum was recorded in the 4000–400 cm^{-1} region by using KBr pellet on a Nicolet Magna 750FT-IR spectrophotometer.

2.4. Computational descriptions

The crystallographic data of compound **1** determined by X-ray were used to calculate electronic band structure of this compound in solid state. The calculations of electronic band structure were made within the density functional theory (DFT) using one of the three nonlocal gradient-corrected exchange-correlation functionals (GGA-PBE) and performed with the CASTEP code [12] which uses a plane wave basis set for the valence electrons and norm-conserving pseudopotential [13] for the core states. Pseudo atomic calculations were performed for Ba-$5s^25p^66s^2$, Zn-$3d^{10}4s^2$, V-$3d^34s^2$ and O-$2s^22p^6$. The number of plane waves included in the basis was determined by cutoff energy $E_c = 450$ eV. The calculating parameters and convergence criterion were

Table 2
Atomic coordinates and equivalent isotropic displacement parameters (Å^2) for $Ba_2ZnV_2O_8$

Atom	x	y	z	U_{eq}
Ba1	0.63811(14)	0.04421(7)	0.23915(17)	0.0113(4)
Ba2	0.14077(14)	0.12918(7)	0.27305(18)	0.0128(4)
Zn	0.7241(3)	0.25014(13)	−0.0016(3)	0.0117(6)
V1	0.8762(4)	0.09120(18)	−0.2464(5)	0.0106(7)
V2	0.5975(4)	−0.17008(18)	0.2636(5)	0.0101(7)
O1	0.5763(16)	0.2557(7)	0.2485(19)	0.012(3)
O2	0.8536(15)	0.1450(7)	0.5078(18)	0.011(3)
O4	0.9491(17)	−0.0328(8)	0.262(2)	0.020(3)
O8	0.6034(17)	−0.1133(8)	0.034(2)	0.019(3)
O6	0.2186(17)	0.2846(8)	0.188(2)	0.018(3)
O3	0.2821(18)	−0.0249(8)	0.233(2)	0.021(3)
O7	0.8688(17)	0.1520(8)	−0.009(2)	0.019(3)
O5	0.5769(16)	−0.1006(8)	0.4665(19)	0.016(3)

[a] $U_{eq} = \frac{1}{3}\sum_i \sum_j U^{ij} a_i^* a_j^* a_i a_j$.

Table 3
Selected bond distances (Å) and angles (°) in $Ba_2ZnV_2O_8$

Bond	Dist.	Bond	Dist.	Bond	Dist.
Ba1–O5^{i}	2.656(4)	Ba2–O6	2.638(13)	Zn–O1^{vii}	1.926(31)
Ba1–O4	2.758(1)	Ba2–O2^{iii}	2.714(38)	Zn–O1	1.943(30)
Ba1–O8^{ii}	2.768(4)	Ba2–O3	2.740(14)	V1–O4^{viii}	1.676(14)
Ba1–O5	2.770(2)	Ba2–O5^{i}	2.776(41)	V1–O2^{ix}	1.753(12)
Ba1–O8	2.852(1)	Ba2–O7^{iii}	2.777(42)	V1–O7	1.762(13)
Ba1–O2	2.870(32)	Ba2–O8^{ii}	2.792(43)	V1–O3^{ii}	1.649(14)
Ba1–O7	2.956(31)	Ba2–O6^{iv}	2.97(2)	V2–O6^{xii}	1.652(16)
Ba1–O3^{ii}	2.997(22)	Ba2–O4^{iii}	3.023(13)	V2–O8	1.686(13)
Ba1–O3	3.027(14)	Zn–O7	1.955(13)	V2–O5	1.688(13)
Ba1–O3^{i}	3.321(22)	Zn–O2^{vii}	1.979(12)	V2–O1^{xii}	1.824(13)
Angle	(°)	Angle	(°)	Angle	(°)
O1^{vii}–Zn–O1	105.71(5)	O3^{ii}–V1–O4^{viii}	105.28(7)	O6^{xii}–V2–O8	111.19(65)
O1^{vii}–Zn–O7	107.01(5)	O3^{ii}–V1–O2^{ix}	107.05(6)	O8–V2–O5	105.23(61)
O1–Zn–O7	114.32(5)	O4^{viii}–V1–O2ix	107.9(6)	O6^{xii}–V2–O1^{xii}	112.18(63)
O1–Zn–O2^{vii}	104.57(49)	O3^{ii}–V1–O7	106.83(6)	O8–V2–O1^{xii}	110.44(60)
O1^{vii}–Zn–O2^{vii}	112.04(49)	O2^{ix}–V1–O7	115.86(6)	O5–V2–O1^{xii}	112.92(59)

Symmetry codes: (i) $1-x, -y, 1-z$; (ii) $1-x, -y, -z$; (iii) $-1+x, y, z$; (iv) $x, 0.5-y, 0.5+z$; (v) $-1+x, y, 1+z$; (vi) $1-x, 0.5+y, 0.5-z$; (vii) $x, 0.5-y, -0.5+z$; (viii) $2-x, -y, -z$; (ix) $x, y, -1+z$; (x) $1+x, y, -1+z$; (xi) $1+x, y, z$; (xii) $1-x, -0.5+y, 0.5-z$; (xiii) $x, y, 1+z$.

set by the default values of CASTEP code [12]. The calculations of linear optical properties were also made in this study. There were 36 conduction bands (CBs) included in the calculation of the imaginary part of the dielectric function, $\varepsilon(\omega)_2$. The $\varepsilon(\omega)_2$ be thought of as detailing the real transitions between occupied and unoccupied electronic states. Since the dielectric constant describes a causal response, the real and imaginary parts are linked by a Kramers–Kronig transform. This transform is used to obtain the real part of the dielectric function, $\varepsilon(\omega)_1$.

3. Results and discussion

3.1. Description of the crystal structure

The crystallographic analysis reveals that the asymmetric independent unit of compound **1** contains two VO_4 tetrahedra, two Ba atoms and one Zn atom. In this structure, there is no detectable disorder among Ba, Zn, and V atoms. The formal oxidation state of 2+, 2+, 5+ may be assigned to Ba, Zn, and V atoms, respectively. The Zn^{2+} cation is tetrahedrally coordinated by four O atoms with the bond distances ranging from 1.926(31) to 1.979(12) Å. The O–Zn–O bond angles are close to 109°, showing that the ZnO_4 tetrahedron is relatively regular. The V–O bond distances can be divided into three groups: the longest one is 1.824(13) Å of the V–μ_3-O, and this type of V–O bonds also can be observed in the compound $SrZnV_2O_7$ (1.822 Å) [8]; the next one is the bond distance (averaged 1.757 Å) of V–μ_2-O, which is consistent with the V–μ_2-O bond distance in the $MM'^{II}_2V_2O_8$ and $M_2M'^{II}V_2O_8$ series; the shortest distance of the V–O_t bond (averaged 1.670 Å) is also in common with $BaZnV_2O_7$ [9] in which V–O_t bonds exist.

The structure of this crystal is composed of 1-D chains of $[ZnV_2O_8^{4-}]_\infty$ separated by Ba^{2+} cations. The $[ZnV_2O_8^{4-}]_\infty$ chain in $Ba_2ZnV_2O_8$ is like a branchy chain composed of ZnO_4 and VO_4 tetrahedra (Fig. 1). The ZnO_4 tetrahedra are connected together to form 1-D straight chains through corner shared O1 atoms. And these O1 atoms are the μ_3-oxo bridges branched by the $V(2)O_4$ groups. In contrast, each $V(1)O_4$ joins two adjacent ZnO_4 tetrahedra through two μ_2-oxo bridges (O2 and O7). The two unique Ba atoms Ba1 and Ba2 are surrounded by ten O atoms and eight O atoms, respectively with the Ba–O bond distances ranging from 2.638(13) to 3.321(22) Å, as shown in Fig. 2. The Ba1 atom links to the surrounding VO_4 and ZnO_4 units through eight O_t atoms of different VO_4 tetrahedra and two μ_2-O atoms (O2, O7), and the Ba2 atom links through six O_t atoms of VO_4 and two μ_2-O atoms(O2, O7). It can be seen that the branchy chains of $[ZnV_2O_8^{4-}]_\infty$ are arranged along *a* and *b* directions alternatively from the view projected along *c*-axis (Fig. 3). The Ba^{2+} cations reside among these branchy chains and join them through Coulombic action of Ba^{2+} cations and O^{2-} anions to form three dimensions framework. The structure type of compound **1** is similar to compound $Ba_2V_3O_9$ or $Sr_2V_3O_9$, which also possesses 1-D $[V_3O_9^{4-}]_\infty$ columns separated by Ba^{2+} or Sr^{2+} cations [14,15].

3.2. Spectral properties of $Ba_2ZnV_2O_8$

The powder XRD pattern of the as-synthesized compound is in well accord with the one simulated on

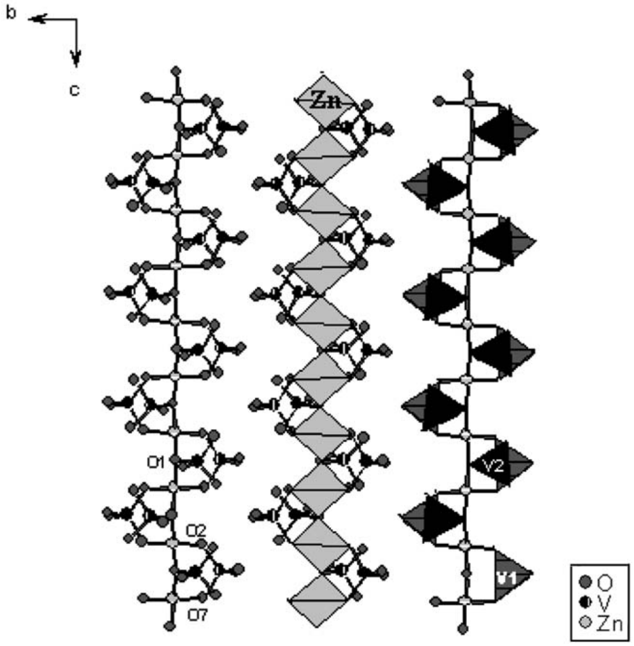

Fig. 1. The $[ZnV_2O_8^{4-}]_\infty$ chains of compound **1**.

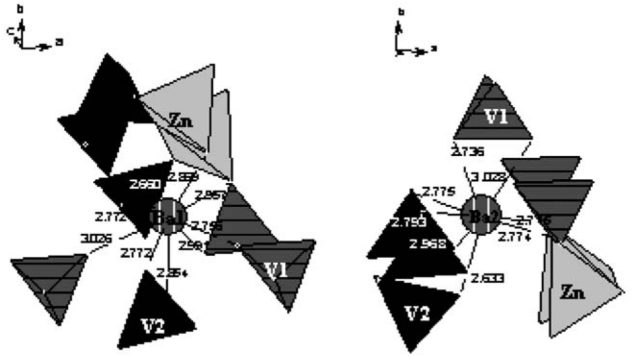

Fig. 2. The coordinated environment of the Ba^{2+} cations.

the basis of the single-crystal structure, indicating the phase purity of the sample. In the IR spectrum of title compound, the strong bands at 910, 876, 844 cm^{-1} are due to the terminal V–O stretching vibrations. The bands at 751, 677 cm^{-1} are attributed to V–O–Zn stretching vibrations and the absorption band with the peak at 453 cm^{-1} probably results from the stretching vibrations of Zn–O. The UV-Vis DRIS spectrum of compound **1** shows that this compound has no absorption ranging from 400 to 1800 nm (Fig. 4). At below 400 nm there is a strong absorption band with one main peak at 319 nm. From the fluorescent spectra of title compound (Fig. 5) we can see that the excitation at 352 nm the sample gives a broad emission band at $\lambda_{max} = 526$ nm. The cut-off edge of the observed absorption is at about 390 nm (3.18 eV) as shown in Fig. 4, and the observed emission peak is at about 526 nm (2.36 eV) as shown in Fig. 5. By comparison these two values, we can deduce that the emitted fluorescence probably originates from defects or excitons due to emission energy of 2.36 eV is less than the optical absorption edge of 3.18 eV.

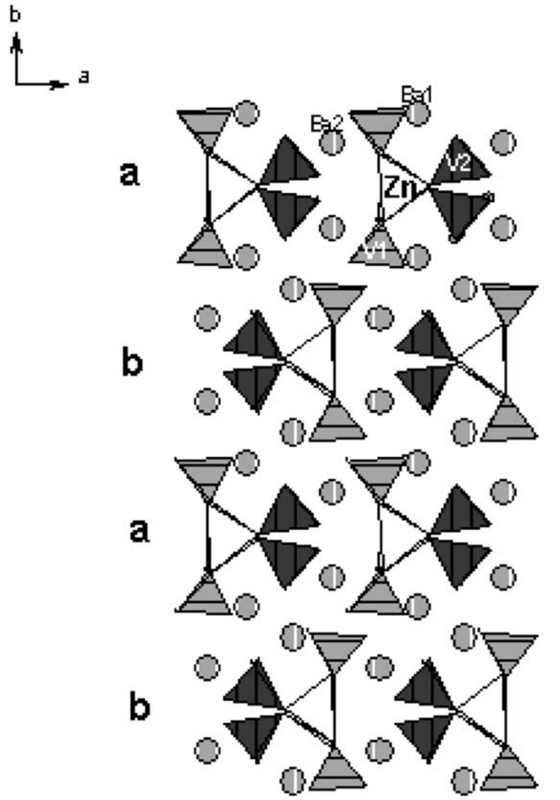

Fig. 3. Projection of the structure of $Ba_2ZnV_2O_8$ in (0 0 1) plane.

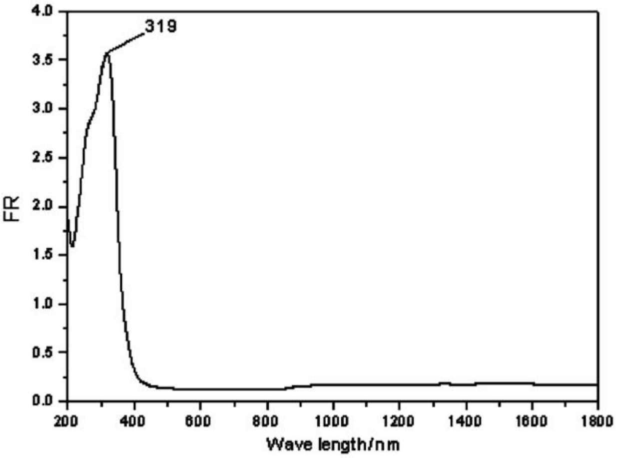

Fig. 4. The UV-Vis DRIS of compound **1**.

3.3. *Band structure, density of states and chemical bond*

The calculated band structure of $Ba_2ZnV_2O_8$ at the Brillouin zone is plotted in Fig. 6. It is observed that the

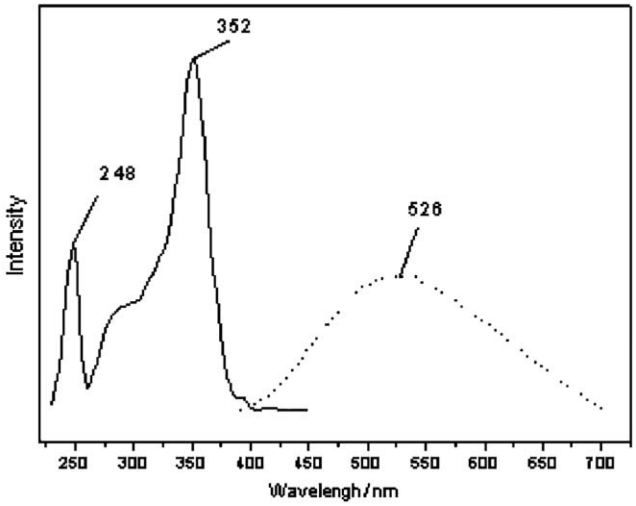

Fig. 5. The excitation spectra (solid line) and emission spectra (dotted line) (excited at 352 nm) of compound **1**.

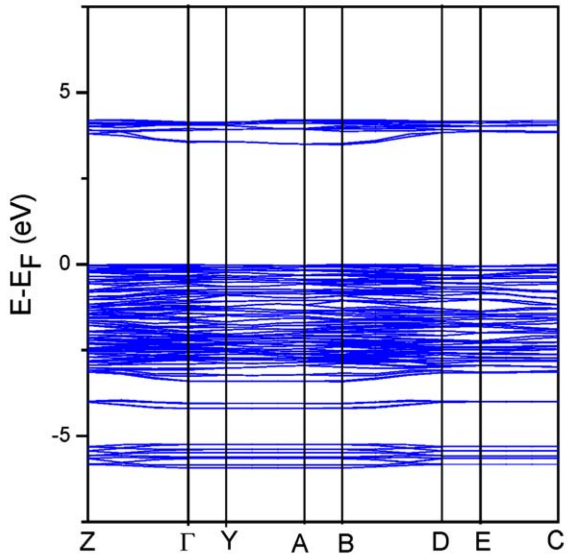

Fig. 6. The band structure for $Ba_2ZnV_2O_8$ crystal (The bands below −7.5 eV have been cut).

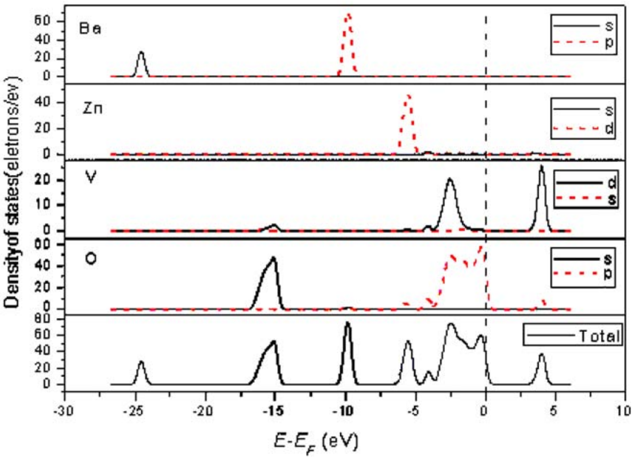

Fig. 7. The partial DOS of $Ba_2ZnV_2O_8$.

top of valence bands (VBs) appears to be very flat, and the lowest energy (3.48 eV) of CBs and the highest energy (0.00 eV) of VB are both localized at B point. The $Ba_2ZnV_2O_8$ shows an insulator with direct band gap of 3.48 eV. The bands can be assigned according to total and partial densities of states (DOS), as plotted in Fig. 7. The states of Ba-5*s* form the VB lying near −25.0 eV, while the states of O-2*s* create the VB ranging from −16.5 and −14.8 eV. The VB between −10.2 and −9.5 eV, and between −6.3 and −5.5 eV, are mostly derived from the Ba-5*p* and Zn-3*d* states, respectively. For the VB between −4.2 eV and the Fermi level (0.0 eV), they are largely formed by the mixings of O-2*p* and V-3*d* states. The top of VB originates from the O-2*p* states, and the CB between 3.5 and 4.2 eV are mainly due to antibonding states between the V-3*d* and O-2*p* states. Accordingly, the absorption edge of UV-Vis DRIS spectrum that is observed at 390 nm (3.18 eV), as shown in Fig. 4, is assigned as the electron transitions from the bonding to antibonding states between the V-3*d* and O-2*p* states. The calculated band gap (3.48 eV, not including shift energy) is as compared with the experiment value of 3.18 eV.

Now, we elucidate the feature of chemical bonding from the nature of total and angular momentum projected DOS. Comparing the total DOS with the angular momentum projected DOS of V-3*d* and O-2*p* states displayed in Fig. 7, we observe that the DOS, the range from about −3.0–0.0 eV, is larger for O-2*p* states (60−electrons/eV) than for V-3*d* states (21 electrons/eV), and the range from −7.0 to −5.0 eV that the DOS is much larger for Zn-3*d* states (48 electrons/eV) than for O-2*p* states (6 electrons/eV). These results show that some electrons from V-3*d* transfer into the VBs and take part in the covalence interactions between V and O atoms, and the electrons from Zn-3*d* transfer into the VBs and take part in the ionic interactions between Zn and O atoms. It is also found that the peaks of total DOS around −25.0 eV and −9.8 eV are completely originated from Ba-5*s* and Ba-5*p* states, which implies that there are pure ionic bonds between Ba and O atoms. The chemical bonding properties are also evidenced from the population analysis. The calculated bond orders of the V–O bond, Zn–O bond and Ba–O bond are from 0.53 to 0.85e, 0.34 to 0.37e and 0.00 to 0.11e in a unit cell of $Ba_2ZnV_2O_8$ (covalence single bond order is generally 1.0e), respectively. Accordingly, we can also say that the covalence strength is stronger for the V–O bond than the Zn–O bond, and ionic strength is stronger for the Ba–O bond than the Zn–O bond in $Ba_2ZnV_2O_8$.

3.4. Optical properties

The calculated imaginary $\varepsilon_2(\omega)$ and the real $\varepsilon_1(\omega)$ parts of the frequency-dependent dielectric function without the scissor-operator approximation are displayed in Fig. 8. The part $\varepsilon_2(\omega)$ can be used to describe the real transitions between occupied and unoccupied electronic states. It is found from the dispersion of the calculated $\varepsilon_2(\omega)$ spectra that there is the first absorption peak localized at about 4.55 (272 nm), 4.58 (270 nm), and 4.91 eV (252 nm), and the second absorption peak localized at about 6.68, 6.53, and 6.74 eV in x, y, z polarization directions for $Ba_2ZnV_2O_8$ crystal, individually. The crystal is transparent while the wavelength is larger than 470 nm or photon energy is less than 2.65 eV. The first and second absorption peaks originate from charge transfers from O to V and to Zn atoms, respectively. Comparing the calculated first absorption peak with the observed absorption peak of power shown in Fig. 4, we can say that the observed peak is originated from O to V charge transfers. The calculated dielectric constant of static case, $\varepsilon(0)$, i.e., $\varepsilon_1(>0)$, is about 2.9410, 2.9491, and 2.8395 in x, y, and z directions, respectively. The dispersion curves of refractive index are also calculated by the relation of $n^2 = \varepsilon$ and plotted in Fig. 9. The refractive index of n_x, n_y, and n_z is 1.7453, 1.7469, and 1.7126 at a wavelength of 1060 nm. The refractive index of $Ba_2ZnV_2O_8$ crystal has not been measured and reported, therefore, our calculated results only compare with the observed results of the other vanadate crystals. It is reported that the observed refractive index of alkali metal or alkaline earth vanadate is generally ranging from 1.7 to 2.0. For example, the average refractive index of $CaMg(VO_4)(OH)$ and $K_2MnV_4O_{12}$ are 1.806 and 1.958 respectively [16,17]. Comparing with the observed refractive index of the other vanadate crystals, our calculated refractive index of the vanadate crystal $Ba_2ZnV_2O_8$ is reasonable and it may be underestimated about 5–10% at static case.

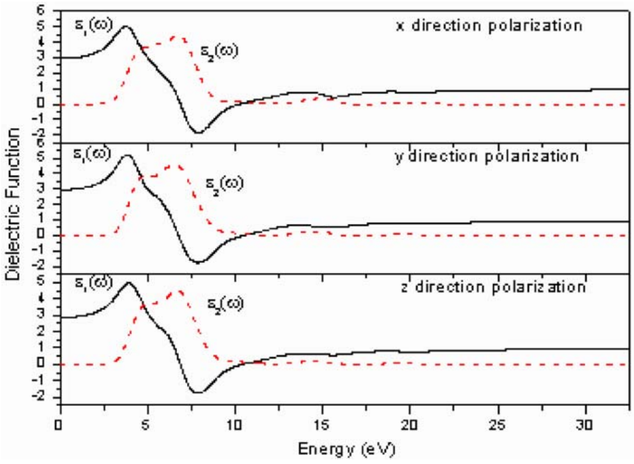

Fig. 8. The calculated dielectric function in different polarization direction of $Ba_2ZnV_2O_8$ crystal.

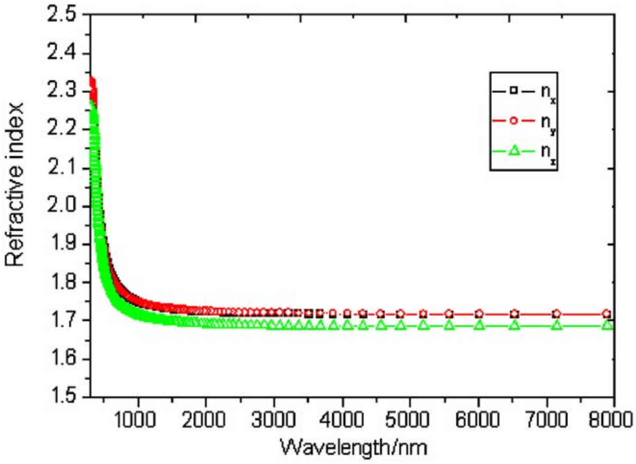

Fig. 9. The calculated dynamic refractive index of $Ba_2ZnV_2O_8$.

4. Conclusions

At the present work, compound $Ba_2ZnV_2O_8$ has been synthesized by high temperature solution reaction, and its crystal structure has been determined. The compound crystallizes in monoclinic system with space group $P2_1/c$. The UV-Vis DRIS and fluorescent spectra have been measured, and they show the lowest energy absorption peak at about 319 nm, and emission peak at 526 nm, respectively. The band structure of the solid state has been calculated using CASTEP code based on the density functional theory, and the obtained results show that the compound is an insulator with direct band gap at about 3.48 eV. The absorption peak that is observed at about 319 nm is assigned as the charge transfers from the O-2*p* to V-3*d* state. The calculated total and partial density of states indicate that the top valence bonds are most contributions from the mixings of O-2*p*, V-3*d*, and Zn-3*d* states, and low conduction bands mostly originate from unoccupied V-3*d* states. The calculated populations show that the interactions between V and O atoms are the significant covalence and those between Zn and O are mostly ionic characters, and the strengths of ionic bond are stronger for the Ba–O bonds than the Zn–O bonds. The linear optical response function of $Ba_2ZnV_2O_8$ crystal has been calculated in terms of the obtained results of band structures. The refractive indices are estimated to be 1.7453, 1.7469, and 1.7126 in x, y, and z direction, respectively.

5. Supplementary material

The supplementary materials have been sent to Fachinformationszentrum Karlsruhe Abt. PROKA, 76344 EggensteinLeopoldshafen, Germany, and can be obtained by contacting the FIZ (quoting the article details and the corresponding CSD numbers: 414009.)

Acknowledgments

This investigation was based on work supported by the National Natural Science Foundation of China under projects 20373073 and 90201015, the Science Foundation of the Fujian Province (No.E0210028, and No. 2002F010), and the Foundation of State Key Laboratory of Structural Chemistry (No. 030060).

References

[1] R. Wichmann, H. Müerller-Buschbaum, Rev. Chim. Miner. 21 (1984) 824–829.

[2] R. Wichmann, H. Müerller-Buschbaum, Rev. Chim. Miner. 23 (1986) 1–7.

[3] R. Vogt, H. Müerller-Buschbaum, Z. Anorg. Allg. Chem. 591 (1990) 167–173.

[4] R. Vogt, H. Müerller-Buschbaum, Z. Anorg. Allg. Chem. 602 (1991) 149–154.

[5] M.V. Postel, H. Müerller-Buschbaum, Z. Anorg. Allg. Chem. 615 (1992) 97–100.

[6] A.G. Nord, P.E. Werner, Z. Kristallogr. 194 (1991) 49–55.

[7] H. Müerller-Buschbaum, O. Schrandt, Z. Naturforsch. Teil B 51 (1996) 817–821.

[8] Yu.A. Velikodnyi, E.V. Myrashova, V.K. Trunov, Kristallografiya 34 (1989) 607–610.

[9] E.V. Murashova, Yu.A. Velikodnyi, V.K. Trunov, ZH. Neorg. Khimii 34 (1989) 1388–1392.

[10] M.V. Postel, H. Müerller-Buschbaum, Z. Anorg. Allg. Chem. 615 (1992) 101–103.

[11] G.M. Sheldrick, SHELXTL-97 Program for Refining Crystal Structure, University of Göttingen, Göttingen, Germany, 1997.

[12] M.D. Segall, P.L.D. Lindan, M.J. Probert, C.J. Pickard, P.J. Hasnip, S.J. Clark, M.C. Payne, J. Phys.: Condens. Matter 14 (2002) 2717.

[13] D.R. Hamann, M. Schluter, C. Chiang, Phys. Rev. Lett. 43 (1979) 1494.

[14] A.-C. Dhaussy, F. Abraham, O. Mentre, H. Steinfink, J. Solid State Chem. 126 (1996) 328.

[15] E.E. Kaul, H. Rosner, V. Yushankhai, J. Sichelschmidt, R.V. Shpanchenko, C. Geibel, Phys. Rev. B 67 (2003) 174417.

[16] T. Witzke, M. Steins, T. Doering, U. Kolitsch, Neues. Jahrb. Miner. Monat. 10 (2000) 444–454.

[17] T. Witzke, S. Zhen, K. Seff, T. Doering, L. Nasdala, U. Kolitsch, Am. Mineral. 86 (2001) 1081–1086.